Pergamon

Ocean Engineering 29 (2002) 1357–1390

OCEAN ENGINEERING

Diffusion reduction in an arbitrary scale third generation wind wave model

W.E. Rogers [a,*], J.M. Kaihatu [a], H.A.H. Petit [b], N. Booij [c], L.H. Holthuijsen [c]

[a] *Oceanography Division, Naval Research Laboratory, Stennis Space Center, MS, USA*
[b] *WL/Delft Hydraulics, Delft, The Netherlands*
[c] *Delft University of Technology, Hydromechanics Section, Stevinweg 1 2628 CN Delft, The Netherlands*

Received 16 March 2001; accepted 27 June 2001

Abstract

The numerical schemes for the geographic propagation of random, short-crested, wind-generated waves in third-generation wave models are either unconditionally stable or only conditionally stable. Having an unconditionally stable scheme gives greater freedom in choosing the time step (for given space steps). The third-generation wave model SWAN ("Simulated WAves Nearshore", Booij et al., 1999) has been implemented with this type of scheme. This model uses a first order, upwind, implicit numerical scheme for geographic propagation. The scheme can be employed for both stationary (typically small scale) and nonstationary (i.e. time-stepping) computations. Though robust, this first order scheme is very diffusive. This degrades the accuracy of the model in a number of situations, including most model applications at larger scales. The authors reduce the diffusiveness of the model by replacing the existing numerical scheme with two alternative higher order schemes, a scheme that is intended for stationary, small-scale computations, and a scheme that is most appropriate for nonstationary computations. Examples representative of both large-scale and small-scale applications are presented. The alternative schemes are shown to be much less diffusive than the original scheme while retaining the implicit character of the particular SWAN set-up. The additional computational burden of the stationary alternative scheme is negligible, and the expense of the nonstationary alternative scheme is comparable to those used by other third generation wave models. To further accommodate large-scale applications of SWAN, the model is reformulated in terms of spherical coordinates rather than the original Cartesian coordinates.

* Corresponding author. Tel.: +1-228-688-4727; fax: +1-228-688-4759.
E-mail address: rogers@nrlssc.navy.mil (W. E. Rogers).

PII: S0029-8018(01)00080-4

Thus the modified model can calculate wave energy propagation accurately and efficiently at any scale varying from laboratory dimensions (spatial scale O(10 m) with resolution O(0.1 m)), to near-shore coastal dimension (spatial scale O(10 km) with resolution O(100 m)) to oceanic dimensions (spatial scale O(10 000 km) with resolution O(100 km).

Keywords: Wind waves; Wave model; Numerical diffusion; Numerical schemes; SWAN; WAM

1. Introduction

Wave action models have been applied at every scale imaginable, from numerical simulations of laboratory experiments to global wave models. Though the dominant processes may vary between applications of differing scale, numerical errors resulting from the discrete approximation of the problem occur at any scale. For any wave model which uses a first order numerical scheme for geographic propagation, diffusion is usually the most serious type of numerical error. Diffusion effects tend to be more severe in the highly nonstationary and nonuniform conditions characteristic of oceanic scales. Numerical diffusion acts to continuously diffuse a feature in a wave field as the feature propagates. For example, in a time series comparison of global model output to data from a deepwater buoy, the diffusion might manifest as an underprediction of energy maxima and overprediction of minima. Diffusion can lead to misinterpretation of results and misguided attempts to improve model skill through alteration of physics and forcing. The finer aspects of a complex numerical model cannot be properly addressed unless the numerical error is sufficiently minimized. Thus, it is readily apparent that a first order scheme—unless applied at extremely fine resolution—is unsuitable for modeling applications in which propagation plays a significant role. Higher-order schemes have therefore been implemented in third-generation wave models. For the WAVEWATCH model (Tolman, 1991), Tolman (1995) uses the "QUICKEST" scheme of Leonard (1979) and Davis and Moore (1982), combined with the "ULTIMATE" total variance diminishing limiter (Leonard, 1991) and reports considerable improvements in numerical accuracy. Bender (1996) improved the numerics of the WAM model (cycle 2, see WAMDI Group, 1988) from first-order to third-order and observed that, in simulations of the Southern Ocean, underpredictions of wave heights due to numerical diffusion are corrected. He notes that this is unsurprising, considering that the area is characterized by swell propagated over long distances. Neu and Won (1990) also look at higher-order schemes in spectral wave models.

All of these models deal with larger scale, nonstationary applications. However, a diffusion-reduction strategy that is appropriate at one scale may not be appropriate for general application. Though it tends to be a greater concern at larger scales, numerical diffusion is not, strictly speaking, affected by scale. In one-dimensional propagation, diffusion by a given numerical scheme (per time step) is simply a function of Courant number, $C_g \Delta t/\Delta x$, and how well the energy feature is resolved by the computational grid (in two dimensions, the angle of incidence of the propagation

direction in relation to the computational grid is also important). Poorly resolved features can exist at any scale. The goal of this present study is to implement a diffusion-reduction strategy for the third generation wave action model SWAN (Booij et al., 1999) that is feasible at all scales. SWAN is well suited for such a study as it contains both deep-water and shallow-water physics.

One work does exist in the literature that aims to reduce numerical error in a wave model inclusive of smaller scales: Lin and Huang (1996) propose three higher-order schemes in their presentation of the "Goddard Coastal Wave Model". The authors report that using these new schemes, diffusion and dispersion are practically zero. Unfortunately, none of these schemes are suitable for diffusion-reduction in an arbitrary scale model. One scheme is derived for a governing equation that is different from that of SWAN (and in fact, should not be used in coastal applications). Mathematical analysis of the other two schemes—denoted "second-order semi-implicit schemes"— shows that they are only first-order. In applications, these schemes appear to have a much broader stability range than the first order scheme used by WAM (WAMDI Group, 1988), but they are quite diffusive, comparable in this respect to the WAM scheme. We were unable to reproduce the accuracy demonstrated in Lin and Huang (1996) using those two schemes.

Though no suitable solution to our particular problem exists in the literature, there does exist a great wealth of research dealing with the accuracy of the numeric approximation of the hyperbolic wave equation for a variety of applications. These works, too numerous to list here, were invaluable in this study.

The SWAN model was originally designed for nearshore applications. The current version of SWAN at the time of this writing (cycle 2, version 40.01) has two shortcomings that make it unsuitable for large-scale applications. Firstly, the model is formulated in Cartesian coordinates; this does not take into account the curvature of the earth's surface, the effects of which are significant at oceanic scales. Secondly, the model employs a first order, upwind, implicit numerical scheme for geographic propagation which is highly diffusive (more so, in general, than the first order, upwind, explicit scheme which is the default scheme of WAM (WAMDI Group, 1988)). This very diffusive scheme was chosen for SWAN due its unconditional stability which allows the use of relatively large time steps with finely resolved (e.g. O(10 m)) computational grids typical of nearshore simulations, thus making it much more efficient on such grids than the WAM model. Also, an unconditionally stable scheme will often be more efficient on curvilinear grids (with varying grid steps in the domain) or spherical grids (with small grid steps near the poles).

Here we investigate the replacement of the first order scheme with higher-order schemes that maintain the basic set-up of SWAN and its operational viability. To that end we choose two schemes which are most suitable for the model from an array of potential alternatives. We implement the replacement schemes and present example applications of the improved model. Simply reformulating the basic action balance equation terms of longitude and latitude (requiring additional refraction-like terms) solves the problem of propagation on a sphere.

2. Model description

The SWAN model ("Simulating WAves Nearshore", Booij et al., 1999) is a third generation wave action model. It is governed by a form of the two-dimensional hyperbolic wave equation, expressed in terms of the wave action density spectrum:

$$N(x,y,\sigma,\theta) = E(x,y,\sigma,\theta)/\sigma, \tag{1}$$

where N is wave action density, E is wave energy density, x and y denote geographic location, σ is the relative frequency, and θ is the direction of propagation. Wave action is propagated in geographic and spectral space, while source and sink terms act on the waves. The action balance equation, in horizontal Cartesian coordinates *(x,y)*, can be written as

$$\frac{\partial}{\partial t}N + \frac{\partial}{\partial x}C_{gx}N + \frac{\partial}{\partial y}C_{gy}N + \frac{\partial}{\partial \sigma}C_{\sigma}N + \frac{\partial}{\partial \theta}C_{\theta}N = \frac{S}{\sigma}. \tag{2}$$

(e.g. Whitham, 1974; Phillips, 1977; Mei, 1983; Hasselman et al., 1973). Here, t denotes time. The first term represents the local rate of change; the second and third terms represent geographic propagation; the fourth term represents changes to relative frequency (e.g. by nonstationary depth or by currents); the fifth term represents refraction (by depth and currents) , and S/σ denotes the total of source and sink terms. The four propagation speeds are shown below (as derived from linear wave theory, e.g. Whitham, 1974; Mei, 1983).

Propagation speed in x-space:

$$C_{gx} = \frac{dx}{dt} = \frac{1}{2}\left[1 + \frac{2kd}{\sinh 2kd}\right]\frac{\sigma k_x}{k^2} + U_x \tag{3}$$

Propagation speed in y-space:

$$C_{gy} = \frac{dy}{dt} = \frac{1}{2}\left[1 + \frac{2kd}{\sinh 2kd}\right]\frac{\sigma k_y}{k^2} + U_y \tag{4}$$

Propagation speed in σ-space:

$$C_{\sigma} = \frac{d\sigma}{dt} = \frac{\partial \sigma}{\partial d}\left[\frac{\partial d}{\partial t} + \bar{U}\cdot\nabla d\right] - c_g\bar{k}\cdot\frac{\partial \bar{U}}{\partial s} \tag{5}$$

Propagation speed in θ-space:

$$C_{\theta} = \frac{d\theta}{dt} = -\frac{1}{k}\left[\frac{\partial \sigma}{\partial d}\frac{\partial d}{\partial m} + \bar{k}\cdot\frac{\partial \bar{U}}{\partial m}\right] \tag{6}$$

Here, $\bar{k} = (k_x,k_y)$ is the wave number with magnitude k (related to σ through the

dispersion relationship of linear wave theory), d is water depth, $\bar{U} = (U_x, U_y)$ is the current velocity, s is the space coordinate in direction θ and m is a coordinate normal to s. The operator d/dt denotes the total derivative along a spatial path of action propagation, and it is defined as:

$$\frac{d}{dt} = \frac{\partial}{\partial t} + C_g \cdot \nabla_{x,y} \tag{7}$$

where $C_g = \bar{k}/k \cdot \partial\sigma/\partial k$ is the group velocity, and $\nabla_{x,y}$ is the horizontal gradient operator. The source/sink terms that act on the action balance equation include wind input, dissipation (by whitecapping, bottom friction, and depth-induced breaking), and nonlinear wave-wave interactions (triads and quadruplets). Detailed description of these terms and how they are implemented in SWAN can be found in Ris (1997) and Booij et al. (1999).

For applications on a large geographic scale, the action balance equation, eq. (2), needs to be reformulated in terms of spherical coordinates by: (a) replacing x and y with longitude (ν) and latitude (λ), (b) replacing the propagation speeds with $\dot{\varphi}, \dot{\lambda}, \dot{\sigma}$ and $\dot{\theta}$ respectively and (c) by replacing $N(x,y,t;\sigma,\theta)dxdy$ with $N(\varphi,\lambda,t;\sigma,\theta)d\varphi d\lambda$. This results in the longitude-latitude formulation of the action balance equation:

$$\frac{\partial}{\partial t}N + (\cos\varphi)^{-1}\frac{\partial}{\partial \varphi}\dot{\varphi}\cos\varphi N + \frac{\partial}{\partial \lambda}\dot{\lambda}N + \frac{\partial}{\partial \sigma}\dot{\sigma}N + \frac{\partial}{\partial \theta}\dot{\theta}N = \frac{S}{\sigma.} \tag{8}$$

where R is the earth's radius and

$$\dot{\varphi} = \left[\frac{1}{2}\left[1 + \frac{2kd}{\sin 2kd}\right]\frac{\sigma k \sin\theta}{k^2} + U_\varphi\right]R^{-1} \tag{9}$$

$$\dot{\lambda} = \left[\frac{1}{2}\left[1 + \frac{2kd}{\sinh 2kd}\right]\frac{\sigma k \cos\theta}{k^2} + U_\lambda\right](R\cos\varphi)^{-1} \tag{10}$$

$$\dot{\sigma} = C_\sigma \tag{11}$$

$$\dot{\theta} = -\frac{1}{k}\left[\frac{\partial\sigma}{\partial d}\frac{\partial d}{\partial m} + \bar{k}\cdot\frac{\partial \bar{U}}{\partial m}\right] - C_s\cos\theta\tan\varphi R^{-1} \tag{12}$$

where θ is the wave direction taken clockwise from geographic east.

The original finite-difference scheme in SWAN for propagation in positive x-direction and positive y-direction is the following first-order (two-level) up-wind scheme (corresponding to (2), ignoring source/sink terms and spectral propagation):

$$\left[\frac{N^{q+1} - N^q}{\Delta t}\right]_{i,j} + \left[\frac{[C_{gx}N]_i - [C_{gx}N]_{i-1}}{\Delta x}\right]_{j,q+1} + \left[\frac{[C_{gy}N]_j - [C_{gy}N]_{j-1}}{\Delta y}\right]_{i,q+1} = 0, \tag{13}$$

where q is a time-level index and i and j are grid counters and Δt, Δx and Δy are

increments in time and geographic space respectively. This is the two-dimensional, first order, backward space, backward time (BSBT) scheme. For combinations of positive and negative *x*-directions and *y*-directions the scheme is obtained by using the proper + and − signs in eq. (13), leading to the four-sweep technique of SWAN. In this case, the implicitness of the scheme makes it unconditionally stable. Thus, the model can be applied in computational grids with small geographic grid spacing without a correspondingly small time step. By comparison, the first order explicit scheme used by WAM (WAMDI Group, 1988) is conditionally stable, though somewhat less expensive per time step (requiring fewer division operations) and somewhat less diffusive (especially for Courant numbers near the stability limit). The BSBT scheme is probably the most diffusive of all commonly used schemes.

3. Alternatives to higher order numerical schemes

Implementation of a higher order scheme is not the only means by which diffusion can be reduced. As diffusion is greatly dependent on geographic resolution, one alternative would be the use of smaller grid size. Increasing resolution has the advantage of decreasing phase error as well as diffusion. This, generally speaking, will lead to fewer numerical oscillations. However, this approach to reducing diffusion in SWAN has two problems that limit its utility:

1. Size limitations: SWAN, as it is currently written, must hold the entire wave action matrix $N(x,y,\sigma,\theta)$ in memory. Thus, there is a practical limitation on how many grid points can be included in the computational grid for a given machine size.
2. Propagation burden: The fraction of computation time spent by SWAN on geographic propagation is generally not large. This may become increasingly true in the future, as more expensive source/sink term formulations are implemented to take advantage of faster computers. If stability requirements and solution techniques are similar for both schemes, then a lower order scheme may be replaced with a much more expensive higher order scheme with only moderate impact on total computation time. By contrast, increasing resolution will have a large impact on total computation time unless the code is altered such that propagation terms are solved on a subdivided grid.

For time-stepping computations, increasing geographic resolution without a corresponding increase in temporal resolution will result in a larger Courant number. In the case of the BSBT scheme, a larger Courant number will, to some degree, offset the benefit of higher geographic resolution. To take an opposite tact, because of the dependence on Courant number, numerical error of the BSBT scheme (and most other schemes) may be decreased by using a smaller time step without a corresponding decrease in geographic step size. However, the dependence of diffusion on time step size is not great for this scheme, so this option can be dismissed.

Replacing the BSBT scheme with another first order scheme would decrease dif-

fusion. For example, the explicit first order upwind scheme (BSFT, stable for Courant number less than one) could be combined with the implicit first order downwind scheme (FSBT, stable for Courant number greater than one) to create an unconditionally stable model which is less diffusive than a model which uses only the BSBT scheme. Though the presentation differs somewhat, this is essentially the approach of Hardy et al. (2000). This type of approach has definite advantages, but for modeling a wider range of applications, it was felt that the additional accuracy of a higher order scheme is required.

It could be argued that the first order explicit scheme, which becomes quite accurate near its stability limit, might be implemented with an adaptive step size. Unfortunately, in the context of a two-dimensional spectral wave model, this approach is inconvenient, and benefit is limited.

4. Discussion: "Wiggles"

Numerical propagation speed depends on the wave length of the Fourier components of the signal. Generally the errors in the propagation speed are largest for the shortest components ($2\Delta x$ waves and somewhat longer). Numerical schemes which do not damp these short components will cause the short waves to become visible as "wiggles" if they are sufficiently present in the solution. It is an ironic fact that a scheme with phase error and no diffusion will generally appear to be worse than a scheme with diffusion and comparable phase error, because the oscillations—which appear much more vividly with the less diffusive scheme—are so obviously non-physical. This seemingly unfair judgement is sometimes justified, as the total variation of error can be as important as the total error. The result of negative wave action (due to the wiggles) is clearly something to avoid. In SWAN, negative wave action is removed during propagation in (σ,θ) space. Such removal obviously compromises wave action conservation. In most applications of SWAN, wiggles will not result in negative wave action, as they occur against a positive background level of energy. Nevertheless, one can easily imagine cases where negative energy is possible, even likely to be generated by the scheme. In an idealized case of propagation through a gap in an obstacle, an illuminated zone is immediately adjacent to a shadowed zone of zero energy. Or an energetic swell field entering an area of calm water may have numerical oscillations leading the edge of the energy front (sometimes called the "shock front").

In general, phase error is dependent on two factors: the Courant number and the resolution of the feature being modeled (the wave form, shock front, etc.). Thus, a scheme which is unconditionally stable may have a practical limitation on Courant number. This limitation is obviously a subjective quantity, unlike a stability criterion. For example, when modeling the propagation of swell across great distances, sufficiently small wiggles might be tolerated because of the greater accuracy of a less diffusive scheme. But in a case where gradients in the wave action field are being used to drive a sediment transport model, wiggles could potentially create non-physical sediment transport patterns. These patterns could be just as problematic as the reduced gradients that would be caused by numerical diffusion.

5. Choice of numerical schemes

5.1. Considerations

Several factors were considered when choosing the replacement schemes:

- Diffusion. This is the greatest deficiency of the existing BSBT scheme. A scheme for which diffusion is not heavily dependent on spatial and temporal resolution is preferred.
- Stability. Unconditional stability is preferred, as it allows more flexibility when choosing a time step size. (As mentioned above, this is especially important when fine geographic resolution is used.)
- Conservation: Conservation of the quantity to be transported is required.
- Numerical dispersion. Minimal numerical oscillation is preferred. Such oscillations (or "wiggles") are dependent on both spatial and temporal resolution.
- Structure. Ideally, the scheme should fit within the general framework of the two-level, up-wind, four-sweep technique that is used in SWAN to solve the discretized action balance equation, Eqs. (2) and (8).
- Expense (per calculation). Though an increase in computational burden is expected, the scheme should not be excessively expensive. A fully implicit scheme requiring additional matrix solutions is undesirable.

5.2. Scheme descriptions

About 40 alternative numerical schemes (for hyperbolic problems) were considered (most of them taken from Petit (1997) who collected these schemes over a period of years, often from unpublished sources). Some were dismissed outright on the basis of the above criteria and considerations. A large group was tested in one-dimensional experiments; most of these were eliminated and a much smaller group was tested in two dimensions.

As most one-dimensional schemes can be generalized to two dimensions in more than one possible manner, it is unhelpful to the reader to present two-dimensional results while only providing a statement of the scheme in one dimension. We state the two-dimensional form used, where appropriate. With regard to judging particular schemes, the one-dimensional problem is a valuable tool for providing a general sense of how the two-dimensional application of a scheme *might* behave, but is much less conclusive than a direct study of the two-dimensional problem. Therefore, we do not present one-dimensional test results here. One-dimensional tests were performed for this study only as a means to eliminate schemes that perform poorly in the simplest tests and therefore are certain to fail miserably in practical applications. It should be stressed that conclusions (e.g. stability requirements, conservation, order of accuracy) derived from testing and/or mathematical analyses of schemes in one dimension do not necessarily apply to the scheme in two dimensions.

There is also the issue of nonuniform Courant number, μ. In the context of a wave action model, this occurs when currents or depths are nonuniform, or when a grid

with variable spacing is used. A two-dimensional scheme which is stable and flux conserving for cases of uniform μ may be less robust in the more general case of nonuniform μ. Unfortunately, mathematical analyses—stability analysis in particular—tend to be difficult, if not impossible, for the general case. Optimistic assumptions can be made based on analyses of the one dimensional scheme with uniform μ. Empirical observation of behavior is particularly useful in such instances.

Using mathematical analysis or empirical study, it is difficult to quantify the accuracy (even relative accuracy) of general schemes, due to the number of degrees of freedom, e.g. the Courant number in two dimensions, the resolution (dimensional or non-dimensional) in two dimensions, severity of μ non-uniformity. Sampling is inevitable.

Each scheme is tested on its own merits, with no consideration of possible enhancements (e.g. filters, limiters). Though it could be argued that this will not necessarily result in the best scheme/enhancement combination, it provides a fair enough attempt.

Of the schemes which were investigated in two-dimensional form, we present five of the most notable examples. The BSBT scheme used by SWAN (cycle 2, version 40) is also described, to provide a baseline. Source/sink terms are neglected for now (the issue is addressed later). In some of these analyses, to quantify numerical error, we use the numerical growth rate (multiplication factor per time step) D, and/or the ratio of physical to numerical celerity, C_n/C. In a general sense, the former is related to stability and diffusion, while the latter is associated with dispersion error and "wiggles".

5.2.1. First order, upwind, implicit (backward space, backward time, BSBT)

Eq. (13) can be written as:

$$(1 + \mu_{x,i,j} + \mu_{y,i,j})N_{i,j}^{q+1} - N_{i,j}^{q} - \mu_{x,i-1,j}N_{i-1,j}^{q+1} - \mu_{y,i,j-1}N_{i,j-1}^{q+1} = 0, \tag{14}$$

where μ_x is the Courant number for propagation in the x direction, $\mu_x = C_{gx}\Delta t/\Delta x$ (C_{gx} is the x-component of the propagation velocity), subscripts i and j indicate grid steps in x and y respectively, and q denotes the time step.

5.2.1.1. Truncation error Eq. (14) effectively solves in the case of constant CFL numbers

$$\begin{aligned}
&\frac{\partial N}{\partial t} + C_{gx}\frac{\partial N}{\partial x} + C_{gy}\frac{\partial N}{\partial y} = \frac{1}{2}C_{gx}^2\Delta t\frac{1+\mu_x}{\mu_x}\frac{\partial^2 N}{\partial x^2} + C_{gx}C_{gy}\Delta t\frac{\partial^2 N}{\partial x\partial y} \\
&+ \frac{1}{2}C_{gy}^2\Delta t\frac{1+\mu_y}{\mu_y}\frac{\partial^2 N}{\partial y^2} + -\frac{1}{6}C_{gx}^3\Delta t^2\frac{3\mu_x^2 + 3\mu_x + 1}{\mu_x^2}\frac{\partial^3 N}{\partial x^3} \\
&-\frac{1}{2}C_{gx}^2C_{gy}\Delta t^2\frac{3\mu_x + 1}{\mu_x}\frac{\partial^3 N}{\partial x^2\partial y} - \frac{1}{2}C_{gx}C_{gy}^2\Delta t^2\frac{3\mu_y + 1}{\mu_y}\frac{\partial^3 N}{\partial x\partial y^2} + \\
&-\frac{1}{6}C_{gy}^3\Delta t^2\frac{3\mu_y^2 + 3\mu_y + 1}{\mu_y^2}\frac{\partial^3 N}{\partial y^3} + O(\Delta t^3)
\end{aligned} \tag{15}$$

By substitution of the CFL numbers the truncation error can be given in terms of Δx, Δy and Δt.

5.2.1.2. Growth rate, dispersion, and stability For the case of uniform propagation speed, the numerical growth rate, D, and the ratio of numerical velocity to actual velocity $C_{g,n}/C_g$ are given by:

$$D^{-2} = [1 + \mu_x(1-\cos(\alpha_x)) + \mu_y(1-\cos(\alpha_y))]^2 + [\mu_x \sin(\alpha_x) + \mu_y \sin(\alpha_y)]^2, \tag{16}$$

$$\frac{C_n}{C} = \frac{\arccos(D\lfloor 1 + \mu_x(1-\cos(\alpha_x)) + \mu_y(1-\cos(\alpha_y))\rfloor)}{\alpha_x\mu_x + \alpha_y\mu_y}. \tag{17}$$

Here, $\alpha_x = k_x \Delta x$ (thus inversely proportional to the number of points per wavelength), where k is the wavenumber vector of the numerical solution (not to be confused with the wavenumber of a wind-wave). In the case where the Courant numbers are uniform, it is apparent from (16) that with $\mu_x \geq 0$ and $\mu_y \geq 0$, that $D^{-2} \geq 1$, and the scheme is therefore unconditionally stable. Experiments have shown that this is likely to be true for the non-uniform case (scheme (14)) as well.

Due to the four degrees of freedom (μ_x, μ_y,α_x, α_y), the expression for D of the two-dimensional problem cannot be presented without a large number of figures. Therefore, the growth rate, D, of the BSBT solution of the one-dimensional problem is shown in Fig. 1. In the context of the two-dimensional wave equation, this figure describes only the special case of energy propagating parallel to the x- or y- axis. However, it is useful for providing a general sense of diffusivity of the scheme relative to two other schemes (below).

5.2.1.3. Conservation Conservation can be proven for the BSBT scheme for the general case of nonuniform μ.

5.2.1.4. Stationary case The stationary case of BSBT can be considered a subset of the nonstationary case: the $\partial/\partial t$ term is equal to zero, and the stationary problem is treated as a nonstationary problem with a single time step of arbitrary size. Analyses for the nonstationary case therefore apply to the stationary case.

5.2.2. Second order, upwind (SORDUP)

For this scheme the spatial derivative is determined as the optimal (most accurate) discretization for the numerical stencil $(i, i-1, i-2)$ using conventional Taylor Series expansion. The stationary case ($\partial/\partial t = 0$) is given as:

$$\left(\frac{3}{2}\mu_{x,i,j} + \frac{3}{2}\mu_{y,i,j}\right)N_{i,j} - 2\mu_{x,i-1,j}N_{i-1,j} + \frac{1}{2}\mu_{x,i-2,j}N_{i-2,j} - 2\mu_{y,i,j-1}N_{i,j-1} + \frac{1}{2}\mu_{y,i,j-2}N_{i,j-2} = 0. \tag{18}$$

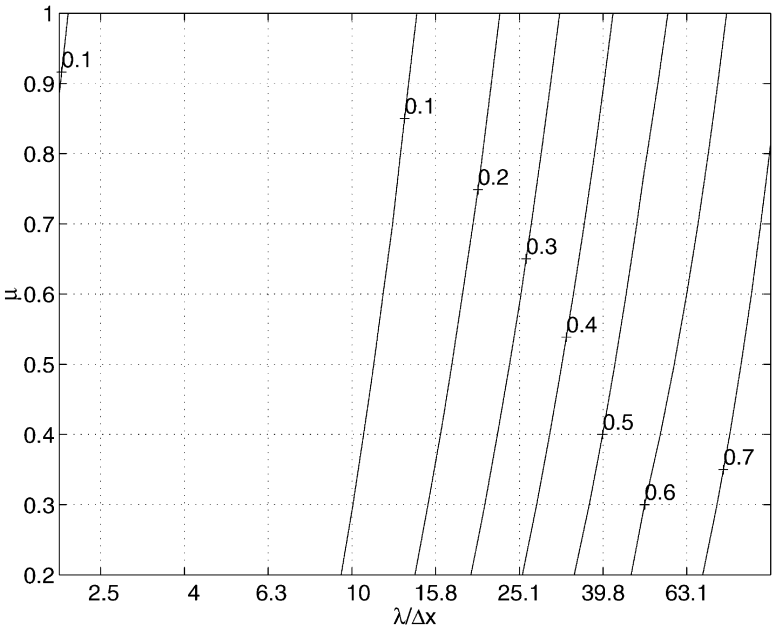

Fig. 1. Numerical growth rate D of the one-dimensional BSBT scheme. Here, λ is the numerical wavelength. Courant number values shown are $\mu \leq 1$, to allow comparison to a conditionally stable scheme (Fig. 3).

Analysis of this stationary, two-dimensional scheme is comparable to the analysis of a nonstationary, one-dimensional scheme with three time levels. The nonstationary case is not given here, as performance of the scheme applied to this type of problem is poor and therefore not considered for implementation in the model.

5.2.2.1. Truncation error For purposes of analysis, the scheme can be re-written as:

$$(1.5\mu_{xy,i,j} + 1.5)N_{i,j} - 2\mu_{xy,i-1,j}N_{i-1,j} + 0.5\mu_{xy,i-2,j}N_{i-2,j} - 2N_{i,j-1} + 0.5N_{i,j-2} = 0, \tag{19}$$

where

$$\mu_{xy} = \frac{\mu_x}{\mu_y} = \frac{C_{gx}\Delta y}{C_{gy}\Delta x}. \tag{20}$$

We find that (19) solves the following differential equation:

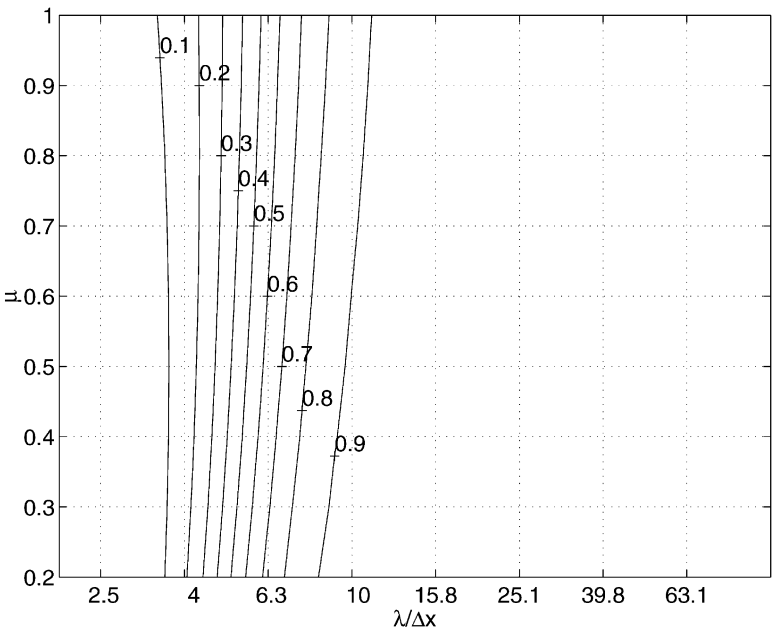

Fig. 2. Numerical growth rate D for the one-dimensional S&L scheme.

$$C_{gx}\frac{\partial N}{\partial x} + C_{gy}\frac{\partial N}{\partial y} = -\frac{1}{3}C_{gx}\Delta x^2(\mu_{xy}^2-1)\frac{\partial^3 N}{\partial x^3}-\frac{1}{4}C_{gx}\Delta x^3(\mu_{xy}^3 + 1)\frac{\partial^4 N}{\partial x^4} + 0(\Delta x^4) \tag{21}$$

5.2.2.2. Stability and amplification factor By study of the amplification factors of the scheme, the unconditional stability of the scheme is made credible for the case of uniform μ.

5.2.2.3. Empirical evidence Applications of the scheme have shown no stability problems. A benchmark test of conservation in two dimensions with non-uniform μ was conducted: a case of an energy signal turning within a control volume (a 90° turn over approximately 150 grid points). This test suggests that the scheme is conservative.

5.2.3. S&L (Q_0=0, Q_1=1/6) (Stelling and Leenderste 1992)

What we refer to as the "S&L" scheme is a cyclic scheme taken from Stelling and Leenderste (1992), the scheme described by "Q_0=0, Q_1=1/6", using their notation. In two dimensions it can be implemented as:

$$\left(1 + \frac{10}{12}\mu_{x,i,j} + \frac{10}{12}\mu_{y,i,j}\right)N_{i,j}^{q+1} = N_{i,j}^{q} - \frac{1}{4}((\mu_x N^q)_{i+1,j} - (\mu_x N^q)_{i-1,j})$$
$$- \frac{1}{4}((\mu_y N^q)_{i,j+1} - (\mu_y N^q)_{i,j-1}) + \frac{1}{12}(15(\mu_x N^{q+1})_{i-1,j} - 6(\mu_x N^{q+1})_{i-2,j} \qquad (22)$$
$$+ (\mu_x N^{q+1})_{i-3,j}) + \frac{1}{12}(15(\mu_y N^{q+1})_{i,j-1} - 6(\mu_y N^{q+1})_{i,j-2}$$
$$+ (\mu_y N^{q+1})_{i,j-3})$$

5.2.3.1. Truncation error The Stelling and Leendertse scheme, as implemented above, with uniform μ_x and μ_y solves the following PDE:

$$\frac{\partial N}{\partial t} + C_{gx}\frac{\partial N}{\partial x} + C_{gy}\frac{\partial N}{\partial y} = -\frac{1}{12}C_{gx}^3\frac{\partial^3 N}{\partial x^3} - \frac{1}{4}C_{gx}^2 C_{gy}\Delta t^2\frac{\partial^3 N}{\partial x^2 \partial y}$$
$$- \frac{1}{4}C_{gy}^2 C_{gx}^2\Delta t^2\frac{\partial^3 N}{\partial y^2 \partial x} - \frac{1}{12}C_{gy}^3\Delta t^2\frac{\partial^3 N}{\partial y^3} - \frac{1}{12\mu_x^2}C_{gx}^4\Delta t^3\frac{\partial^4 N}{\partial x^4} - \frac{1}{12\mu_x^2}C_{gx}^3 C_{gy}\Delta t^3\frac{\partial^4 N}{\partial x^3 \partial y} \qquad (23)$$
$$- \frac{1}{12\mu_y{}^2}C_{gy}^3 C_{gx}\Delta t^3\frac{\partial^4 N}{\partial y^3 \partial x} - \frac{1}{12\mu_y^2}C_{gy}^4\Delta t^3\frac{\partial^4 N}{\partial y^4} + O(\Delta t^4)$$

The order of consistency shows that the phase error is second order in Δt whereas diffusion is third order. This is an obvious improvement over the BSBT scheme. Moreover, for smaller Courant numbers (say, for $[\mu_x, \mu_y] < 3$), this diffusion dampens the higher wavenumbers (of the propagating feature) much better than the low wavenumbers, thus reducing the wiggles. Wiggles are therefore sufficiently smoothed that they are hardly noticeable (except in extreme cases).

5.2.3.2. Growth rate and dispersion (stability and oscillations) Expressions for growth rate, D, and relative celerity $C_{g,n}/C_g$ were calculated, but are quite long and are omitted here. Experimentation with a large number of possible input values for the derived expression for D yielded no unstable combinations. Therefore, the scheme is very likely unconditionally stable.

The scheme can be made stationary by the assumption $N_{i,j}^{q+1} = N_{i,j}^{q}$. However, this discretization cannot be considered a subset of the nonstationary scheme and may be unstable. Also, it is important to note that the numerical stencil of such a stationary S&L scheme includes downwind points, which is incompatible with the up-wind set-up of SWAN. The stationary version of the scheme will therefore not be considered further. Fig. 2 shows the growth rate, D, for the one-dimensional application of the scheme.

5.2.3.3. Empirical evidence As with the BSBT scheme, experience with using this scheme suggests that it is unconditionally stable for cases of non-uniform μ. How-

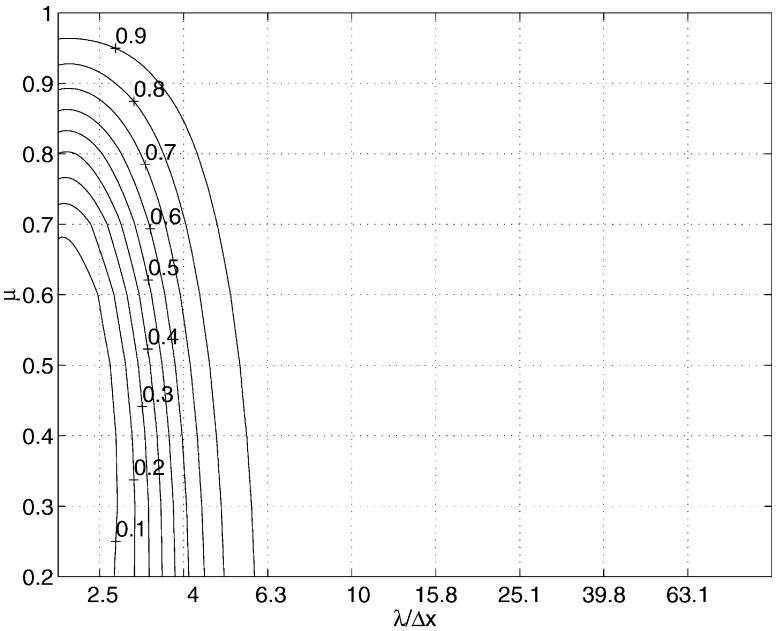

Fig. 3. Growth rate D of the one-dimensional BCML (n=3) scheme.

ever, because of the numerical oscillations, there is a practical limitation to time step size with this scheme. The maximum usable Courant number is a very subjective number depending on the tolerance of the model user, the severity of the "shock front" or comparable feature in the wave action field, and the resolution of the feature. In field applications, the largest acceptable Courant number can be as low as 2.0 or as high as 10.0. Under more ideal conditions (e.g. propagation past a semi-infinite breakwater in deep water), $\mu \approx \infty$ can often be used.

The benchmark test for conservation of action suggests that the scheme is perfectly conserving for the general case of non-uniform μ.

5.2.4. Box

5.2.4.1. One-dimensional implementation The "Box" scheme, used the solve the one dimensional wave equation uses the following finite differencing (Preissmann, 1961):

$$\frac{\partial N}{\partial t} \approx \frac{1}{2}\left(\frac{N_i^q - N_i^{q-1}}{\Delta t} + \frac{N_{i-1}^q - N_{i-1}^{q-1}}{\Delta t}\right) \tag{24}$$

$$\frac{\partial N}{\partial x} \approx \frac{1}{2}\left(\frac{N_i^q - N_{i-1}^q}{\Delta x} + \frac{N_i^{q-1} - N_{i-q}^{q-1}}{\Delta x}\right) \tag{25}$$

The scheme is unconditionally stable and accurate to second order in this one-dimensional form. This scheme is unusual because it does not have any diffusion (D=1;

no even-ordered derivatives in the truncation error). In itself this is a good property as the amplitudes of each Fourier components of the initial condition are preserved if applied on the simple wave equation (constant μ). Unfortunately the scheme does have phase errors, resulting in "wiggles". The oscillations are much more noticeable than they would be if the scheme did have diffusion. Thus, when and where oscillations do occur, the total lack of diffusion might be considered a drawback.

This higher order scheme has the attractive feature of a compact numerical stencil, making it suitable for applications along boundaries (both internal and external).

5.2.4.2. Two-dimensional implementation We use a two-dimensional implementation which might more accurately be called a "cube" scheme, where each derivative is calculated from the eight points on an upwind-oriented cube:

$$\frac{\partial N}{\partial t} \approx \frac{1}{4}\left(\frac{N_{i,j}^{q}-N_{i,j}^{q-1}}{\Delta t}+\frac{N_{i-1,j}^{q}-N_{i-1,j}^{q-1}}{\Delta t}+\frac{N_{i,j-1}^{q}-N_{i,j-1}^{q-1}}{\Delta t}+\frac{N_{i-1,j-1}^{q}-N_{i-1,j-1}^{q-1}}{\Delta t}\right), \tag{26}$$

$$\frac{\partial N}{\partial x} \approx \frac{1}{4}\left(\frac{N_{i,j}^{q}-N_{i-1,j}^{q}}{\Delta x}+\frac{N_{i,j}^{q-1}-N_{i-1,j}^{q-1}}{\Delta x}+\frac{N_{i,j-1}^{q}-N_{i-1,j-1}^{q}}{\Delta x}+\frac{N_{i,j-1}^{q-1}-N_{i-1,j-1}^{q-1}}{\Delta x}\right), \tag{27}$$

$$\frac{\partial N}{\partial y} \approx \frac{1}{4}\left(\frac{N_{i,j}^{q}-N_{i,j-1}^{q}}{\Delta y}+\frac{N_{i,j}^{q-1}-N_{i,j-1}^{q-1}}{\Delta y}+\frac{N_{i-1,j}^{q}-N_{i-1,j-1}^{q}}{\Delta y}+\frac{N_{i-1,j}^{q-1}-N_{i-1,j-1}^{q-1}}{\Delta y}\right). \tag{28}$$

It can be shown that, with this two-dimensional implementation, the scheme remains second order accurate. Conservation can be proven by constructing the Box scheme using a finite volume method. It can be proven for the case of uniform μ that the scheme is unconditionally stable and has no diffusion. Extensive applications suggest that this also holds true in the case of non-uniform μ. Not surprisingly, the unusually severe numerical oscillations of the Box scheme are also evident in two dimensions. The unattractive prospect of a numerical filter may be unavoidable in an implementation of this scheme.

5.2.5. NISL (non-interpolating, semi-Lagrangian Lax–Wendroff scheme)

This scheme works by scanning back along the characteristic line to the previous time level. Since the characteristic line typically does not terminate on a grid node at the previous time level, a finite differencing scheme (Lax–Wendroff) is used—in lieu of interpolation—to make the appropriate correction to the terminus value.

5.2.5.1. Nonstationary implementation The NISL scheme, in two dimensions, is stated by Olim (1994) as:

$$N^{q}_{i,j} \approx N^{q-1}_{i-\psi,j-\xi}(1-\mu^2_{rx}-\mu^2_{ry}) + \frac{\mu_{rx}\mu_{ry}}{4}(N^{q-1}_{i-\psi-1,j-\xi-1} + N^{q-1}_{i-\psi+1,j-\xi+1} - N^{q-1}_{i-\psi+1,j-\xi-1} - N^{q-1}_{i-\psi-1,j-\xi+1}) + \frac{\mu_{rx}}{2}[N^{q-1}_{i-\psi-1,j-\xi}(1+\mu_{rx}) - N^{q-1}_{i-\psi+1,j-\xi}(1-\mu_{rx})] + \frac{\mu_{ry}}{2}[N^{q-1}_{i-\psi,j-\xi-1}(1+\mu_{ry}) - N^{q-1}_{i-\psi,j-\xi+1}(1-\mu_{ry})], \quad (29)$$

where μ_{rx} is the residual Courant number in x-space, $(C_{gx}\Delta t/\Delta x - \psi)$; ψ is the nearest integer to $\mu_x = (C_{gx}\Delta t/\Delta x)$; μ_{ry} is the residual Courant number in y-space, $(C_{gy}\Delta t/\Delta y - \xi)$; ξ is the nearest integer to $\mu_y = (C_{gy}\Delta t/\Delta y)$.

5.2.5.2. Nonstationary performance This scheme generally performed as well as other higher order schemes (e.g. S&L, Box) for CFL values less than one. For larger values, results are more impressive: the scheme actually becomes more accurate as CFL increases. However, it was found that the scheme is conditionally stable (e.g. the scheme is unstable for $\mu_{xr} = \mu_{xr} = 0.5$, $\alpha_x = \alpha_y = \pi/2$). The stability requirements of eq. (29) were judged so problematic that the scheme was dropped from the test group. (We note that it was later found that Olim's one-dimensional scheme can be extended to two dimensions in such a way that the unconditional stability is preserved (H. Petit, personal communication)).

5.2.5.3. Stationary implementation This is essentially the one-dimensional form given by Olim (1994), with the time variable replaced by a second space variable. In cases where $C_{gx}/\Delta x \geq C_{gy}/\Delta y$, the scheme is:

$$N_{i,j} \approx N_{i-p,j-1} - 1/2(\mu_{xy}-p)(N_{i-p+1,j-1} - N_{i-p-1,j-1}) = 1/2(\mu_{xy}-p)^2(N_{i-p+1,j-1} - 2N_{i-p,j-1} - N_{i-p-1,j-1}), \quad (30)$$

where $\mu_{xy} = \dfrac{C_{gx}\Delta y}{C_{gy}\Delta x}$ and p is the nearest integer to μ_{xy}.

In cases where $C_x/\Delta x < C_y/\Delta y$, the scheme is:

$$N_{i,j} \approx N_{i-1,j-p} - 1/2(\mu_{xy}-p)(N_{i-1,j-p+1} - N_{i-1,j-p-1}) + 1/2(\mu_{xy}-p)^2(N_{i-1,j-p+1} - 2N_{i-1,-p} - N_{i-1,j-p-1}), \quad (31)$$

where $\mu_{xy} = \dfrac{C_{gy}\Delta x}{C_{gx}\Delta y}$.

In (31), the first subscript is analogous to the time subscript of the one-dimensional nonstationary scheme and the second subscript is analogous to the space subscript of that scheme. Eq. (31) has an explicit diffusion term. This is potentially convenient for dealing with the so-called "Garden Sprinkler Effect" (GSE), (SWAMP Group, 1985, Booij and Holthuijsen,1987). The scheme is unconditionally stable.

Unfortunately, the scheme, as stated above, has little value for solving problems

of nonuniform μ because it assumes that μ_{xy} does not change along the characteristic line. If μ_{xy} does change, the scheme essentially "looks back" to the incorrect location. To solve the problem correctly, it is necessary to integrate propagation along a curved characteristic (for example, by ray tracing along a subdivided grid). Thus, implementation of Eqs. (30) and (31) in SWAN is ruled out, though it might be possible to implement a similar, but more generally correct, procedure sometime in the future.

5.2.5.4. Stationary performance The benchmark (nonuniform C_g) test of conservation bears out concerns regarding performance with nonuniform μ: the flux out of the control volume equals approximately 23% of flux into the control volume.

5.2.6. BCML (n=3) (backward characteristic method, Lagrangian interpolation)

It was felt that a higher order, conditionally stable scheme should be investigated in detail along with the unconditionally stable schemes described above. The BCML (n=3) scheme was chosen for this. The BCML method is described in Petit (1997) in one dimension for all values of n as:

$$N_j^{q+1} = \sum_{i=-n}^{n-1} \left(\prod_{m=-n, m\neq i}^{n-1} \frac{m+\mu}{m-i} \right) N_j^{q+i} \tag{32}$$

For n=2, this is the "QUICKEST" scheme (Leonard, 1979; Davis and Moore, 1982), notable because the WAVEWATCH model (Tolman, 1995) uses this scheme, along with the "ULTIMATE" total variance diminishing limiter (Leonard, 1991).

One possible implementation of BCML (n=3) in two dimensions with nonuniform μ is:

$$N_{i_1,i_2}^{q+1} - \sum_{j_1=-3}^{2} \sum_{j_2=-3}^{2} \left(\prod_{\substack{m=-3 \\ m\neq j_1}}^{2} \frac{m+\mu_{x,i_1,i_2}}{m-j_1} \right) \left(\prod_{\substack{n=-3 \\ n\neq j_2}}^{2} \frac{n+\mu_{y,i_1,i_2}}{n-j_2} \right) \frac{\mu_{x,i_1+j_1,i_2}\mu_{y,i_1,i_2+j_2}}{\mu_{x,i_1,i_2}\quad\mu_{y,i_1,i_2}} N_{i_1+j_1,i_2+j_2}^{q} = 0. \tag{33}$$

5.2.6.1. Truncation error and stability: uniform μ We analyzed truncation error and stability only for the case of uniform μ, where

$$\frac{\mu_{x,i_1+j_1,i_2}\mu_{y,i_1,i_2+j_2}}{\mu_{x,i_1,i_2}\quad\mu_{y,i_1,i_2}} = 1 \tag{34}$$

This less general form of (33) solves the differential equation

$$\frac{\partial N}{\partial t} + C_{gx}\frac{\partial N}{\partial x} + C_{gy}\frac{\partial N}{\partial y} = -\frac{1}{720}\Delta x^5 C_{gx} \prod_{\substack{m=-3 \\ m\neq 0}}^{2} (\mu_x + m)\frac{\partial^6 N}{\partial x^6}$$

$$-\frac{1}{720}\Delta y^5 C_{gy} \prod_{\substack{m=-3 \\ m\neq 0}}^{2} (\mu_y + m)\frac{\partial^6 N}{\partial y^6} - \frac{1}{1680}\Delta x^6 C_{gx}(2\mu_x - 1) \prod_{\substack{m=-3 \\ m\neq 0}}^{2} (\mu_x \qquad (35)$$

$$+ m)\frac{\partial^7 N}{\partial x^7} - \frac{1}{1680}\Delta y^6 C_{gy}(2\mu_y - 1) \prod_{\substack{m=-3 \\ m\neq 0}}^{2} (\mu_y + m)\frac{\partial^7 N}{\partial y^7} + O(\Delta x^7) + O(\Delta y^7)$$

This two-dimensional equation is therefore fifth order accurate. The stability condition is: $0 \leq \mu_x \leq 1 \wedge 0 \leq \mu_y \leq 1$.

Expressions for D and C_n/C were also derived, but are omitted here for the sake of brevity. Fig. 3 shows the growth rate, D, of the one dimensional application of the scheme. Though not the general (two-dimensional) case, comparison with Figs. 1 and 2 provide a general sense of diffusivity relative to the other schemes. It is apparent that the BCML(n=3) method has far less diffusion than the other schemes considered. Only the short wave components are damped out rapidly.

5.2.6.2. Conservation in one dimension It can be shown that the BCML (n=3) scheme is conservative for the case of uniform μ, and approximately conservative for the case of mildly varying μ.

5.2.6.3. Conservation in two dimensions Because the scheme is relatively complex, we do not attempt to prove conservation in two dimensions.

5.2.6.4. Empirical evidence Tests indicate that the scheme is conservative for the case of uniform μ and conditionally stable for the general cases. We applied the stability range (derived for the case of uniform μ) to the benchmark tests which included non-uniform μ and never encountered stability problems. The benchmark conservation test indicates that conservation behavior of the two-dimensional scheme is similar to that of the one-dimensional scheme: approximate conservation with nonuniform μ.

5.2.6.5. General comments Some general comments can be made regarding the BCML (n=3) scheme:

1. The conditional stability of the scheme makes it more appropriate for large-scale applications. This is an acceptable limitation, due to the availability of other schemes that can be used at smaller scales.
2. The scheme is fifth order accurate, but because it has a 36-point stencil and numerous division operations, it is too expensive for implementation in SWAN with

present-day computer technology. The impressive accuracy of the scheme (examples shown below) offers a demonstration of what may be possible in the future with schemes such as this one.

3. Conservation error exists with the scheme for non-uniform μ. This error will be negligible for most wave model applications. If perfect conservation is needed, there may exist means to achieve this (e.g. by solving the governing equation using Finite Volume Methods rather than by finite differencing).

6. Simple applications

Here, we detail two of the more notable applications used in the empirical analysis mentioned above. Both scenarios can be considered diffusion-prone (relative to typical model applications). One is representative of large-scale cases, and the other is representative of smaller scale cases.

6.1. Nonstationary example: two-dimensional spike propagation

The propagation of a two-dimensional spike is used to represent the travel of a swell system across an ocean. The narrow shape of the spike makes it a severe test case, very prone to the effects of diffusion and dispersion. Only one spectral bin is used per spike, so alteration of the shape of individual spikes during propagation is purely artificial. The spike is defined by:

$$N(x,y) = [\cosh(\Gamma/r)]^{-1}, \tag{36}$$

where r is a representative radius of the spike, and Γ is the radial distance from the spike center.

Numerics are affected by Courant number, the resolution of the spike, and the angle of propagation; many combinations were used. Sample cases are shown in Fig. 4. The initial shape and location of the four spikes are shown in the lower left corner. The four spikes are propagated at angles of 0, 15, 30, and 45 degrees. The parameter "*A*" (shown at the end location of each spike) indicates the fraction of spike amplitude retained, a rough measure of diffusion. The problem is non-dimensionalized and solved in terms of Courant numbers $C_{gx}\Delta t/\Delta x$ and $C_{gy}\Delta t/\Delta y$. Thus, spatial scale is arbitrary. Model parameters for the cases shown in this figure are: $C_g\Delta t/\Delta s$=0.75, Δx=Δy=0.1, where $C_g = \sqrt{C_{gx}^2 + C_{gy}^2}$ and $\Delta s = \sqrt{\Delta x^2 + \Delta y^2}$. Results are generally in agreement with the results of mathematical analysis. For example,

- the NISL scheme becomes more accurate as (μ_x, μ_y) increases, and is the most accurate scheme for (μ_x, μ_y) > 2.
- oscillations are generally more noticeable with the Box scheme than with other schemes.
- BCML(n=3) is the most accurate scheme (for (μ_x, μ_y) < 1)
- The Box scheme is less diffusive than the S&L scheme.

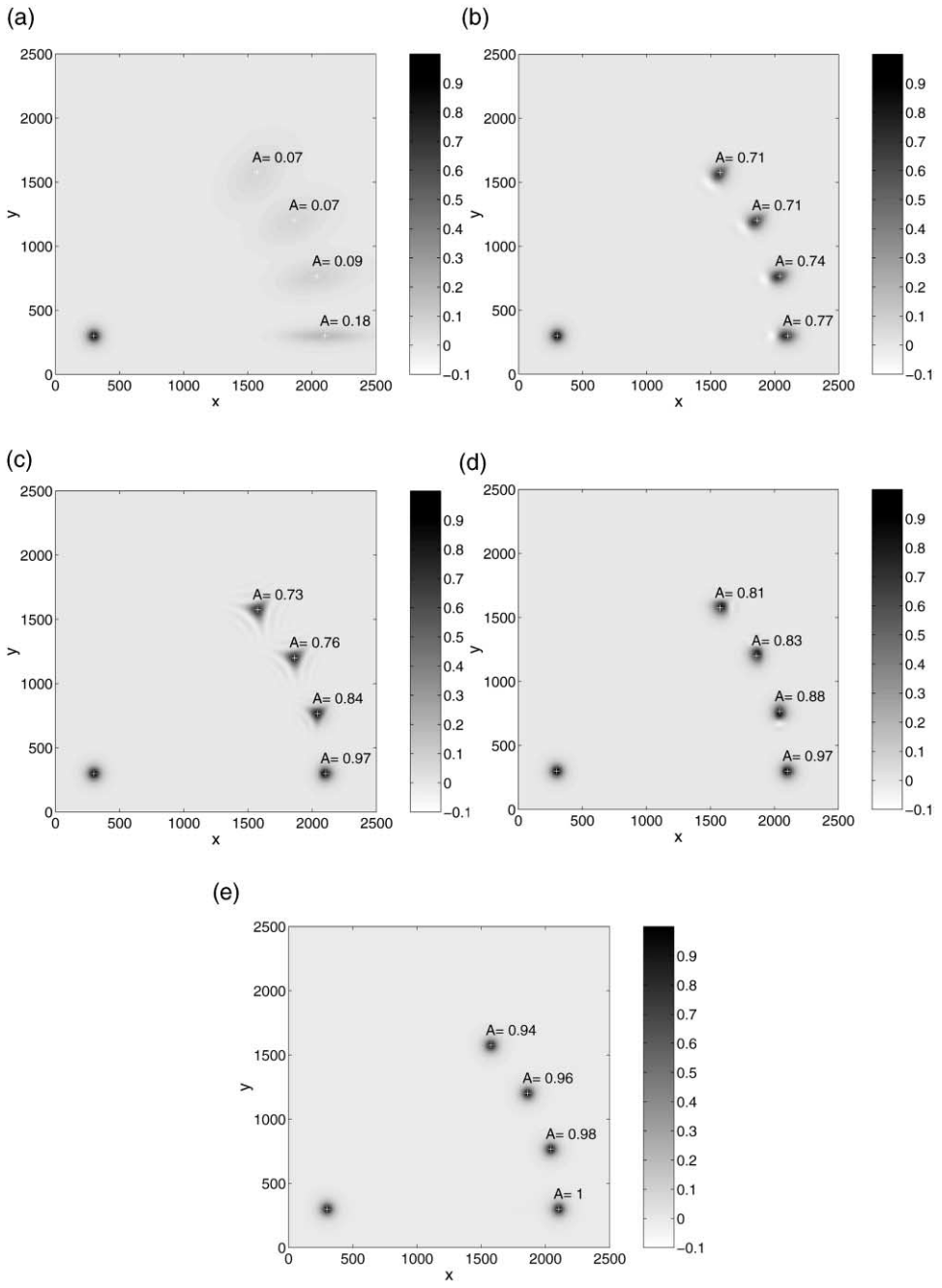

Fig. 4. Results of two-dimensional spike propagation test using the a) BSBT, b) S&L, c) Box, d) NISL and e) BCML (n=3) schemes. The conserved quantity, wave action, is shown. Length scales are of arbitrary units; e.g. if units of km, the problem can be interpreted as swell propagation across an ocean.

- S&L is much less diffusive than BSBT, much faster than BCML(n=3), and has less obvious "wiggles" than Box (mostly due to the diffusion of S&L).

There was initially some concern that the omission of "off-axis" points in the two dimensional implementation of the S&L scheme (eq. (22)) would lead to distortion of the signal. While some distortion is noticeable, it is no worse than the BOX scheme (which does include "off-axis" points).

6.2. Stationary example: propagation past a breakwater

An idealized submerged breakwater is simulated by specifying the wave height at an open boundary (x=0) H=1 for $y<98$ and $y>104$ H=2 for 98 <= y <= 104, (a rectangular wave energy signal superimposed on a background wave field), where x and y are nondimensionalized by Courant number and H is the dimensionless wave height. At the downwave open boundary (x=100), the numerical solution can be compared to an exact analytical solution. In this case, numerics are affected by geographic resolution and angle of propagation; various combinations were used for comparisons. Sample comparisons are shown in Fig. 5. Spatial resolution used in this particular case are: Δx=1, Δy=2. Spatial units are nondimensionalized by $C_{gx}\Delta t/\Delta x$ and $C_{gy}\Delta t/\Delta y$ (Δt is a dummy variable in true stationary computations). Angle convention is defined by: propagation at 0° being parallel to the x-axis (+x), and propagation at 90° being parallel to the y-axis (+y). Note that in the context of a wind-wave model, this is an extreme test case. Because of the steep gradients of the problem, both diffusion and wiggles are greatly exaggerated relative to a more typical wave-modeling problem.

The S&L scheme is included in the comparison of the stationary schemes; the scheme was run in nonstationary mode until steady state was reached. A relatively small time step was used; therefore the S&L results used in these stationary comparisons are an optimistic representation of performance that can be expected from the scheme at the resolutions tested.

Results are as expected: the higher order schemes are much less diffusive, though wiggles are visible in the solutions. Of these schemes, the S&L scheme has the least noticeable phase speed error, but is relatively inefficient (because this is a stationary problem).

6.3. Implementation

Through side-by-side comparisons and the process of elimination described (in part) above, the schemes chosen for implementation were the S&L scheme (primarily for nonstationary applications) and the SORDUP scheme (for stationary applications). These two schemes have been added to the original code, alongside the BSBT scheme. Near boundaries and obstacles, the model reverts to the first order scheme.

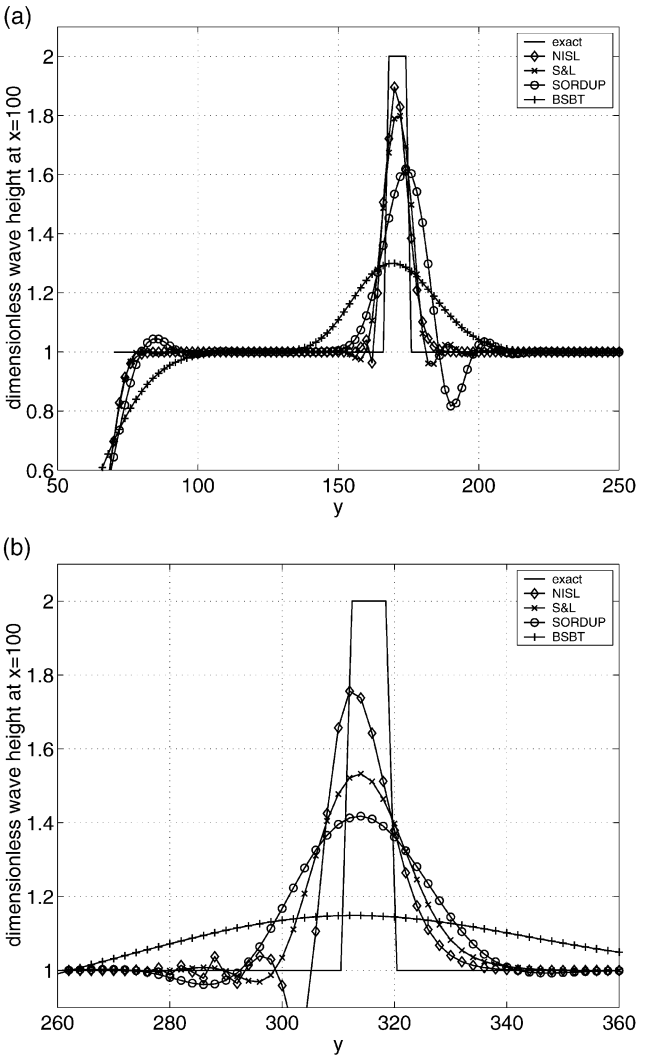

Fig. 5. Example two-dimensional, stationary application: propagation of wave energy past a gap in a breakwater. Shown are the results along a transect parallel to gap at 100 units distance behind the gap for propagation angles 35° (left figure) and 65° (right figure). Length scales are of arbitrary units; e.g. meters.

6.3.1. Nonstationary

In terms of computation time, the nonstationary model remains efficient with the S&L scheme. Use of the scheme (along with GSE-correcting diffusion described below) typically results in a 40%–50% increase in computation time per time step. As discussed above, there is less freedom to use large time steps with the S&L scheme (as compared to the BSBT scheme). In some situations (particularly with finely resolved grids), the limit on time step-size will result in considerably greater

computation time. This is not a serious problem, since small-scale, high resolution problems are generally treated as stationary cases, for which a third scheme can be used (see following section).

6.3.2. Stationary

The second order, upwind (SORDUP) scheme, implemented for use as the primary stationary scheme, is not significantly more expensive than the BSBT scheme. In some cases, computation time is actually reduced due to faster convergence (this refers to iterations used by SWAN which are not directly related to geographic propagation). The "wiggles" of the SORDUP scheme are the only potential drawback, and these oscillations will be negligible for most applications. (We note, however, that it is possible to eradicate wiggles from the SORDUP scheme by using an extension of the scheme which is more diffusive (only first order accurate), yet still less diffusive than the BSBT scheme.)

No true stationary version of the S&L scheme was implemented. It is possible to employ the nonstationary S&L-based model, with constant forcing, until steady state is achieved. However, the number of time steps required by this pseudo-stationary model is proportional to the number of grid points along the direction of propagation. Since the SORDUP scheme does not suffer this limitation, it is more efficient for stationary cases with a moderate (or larger) number of grid points.

6.4. The "garden sprinkler effect"

6.4.1. Nonstationary

With the reduced diffusion of the S&L scheme, the well known "garden sprinkler effect" (GSE) (e.g. SWAMP Group, 1985) becomes noticeable. The garden sprinkler effect occurs when spectral discretization is too coarse for the scale of propagation. It manifests as nonphysical discontinuities in the wave field which appear as natural dispersion occurs. This problem can be countered by using a fine spectral discretization. When this is computationally infeasible, one can use the procedure of Booij and Holthuijsen (1987). This procedure operates by diffusing wave energy a) in the direction of wave propagation (to counter the effect of frequency discretization; see (41)) and b) normal to the direction of wave propagation (to counter effect of directional discretization; see (42)). In effect, diffusion is used to approximate the natural dispersion of continuous spectra. The resulting wave action balance equation (omitting source terms and spectral propagation terms), is

$$\frac{\partial}{\partial t}N(x,y,t) + \frac{\partial}{\partial x}[C_{gx}N(x,y,t) - D_{xx}\frac{\partial}{\partial x}N(x,y,t)] + \frac{\partial}{\partial y}[C_{gy}N(x,y,t) - D_{yy}\frac{\partial}{\partial y}N(x,y,t)] - 2D_{xy}\frac{\partial^2}{\partial x \partial y}N(x,y,t) = 0, \tag{37}$$

where

$$D_{xx} = D_{ss}\cos^2\theta + D_{nn}\sin^2\theta, \tag{38}$$

$$D_{yy} = D_{ss}\sin^2\theta + D_{nn}\cos^2\theta, \tag{39}$$

$$D_{xy} = (D_{ss} - D_{nn})\sin\theta\cos\theta, \tag{40}$$

$$D_{ss} = \Delta C_g^2 T/12, \quad \text{and} \tag{41}$$

$$D_{nn} = C_g^2 \Delta\theta^2 T/12. \tag{42}$$

where T is the wave age of the wave component considered (the time elapsed since the generation of the bulk of the energy of the wave component), $\Delta\bar{C}$ is the difference in propagation speed across the spectral frequency bin and $\Delta\theta$ is the directional resolution. The first-order derivative terms comprise of the unmodified governing equation, while the second-order derivative terms are the GSE-correcting modifications.

Simple, explicit finite differencing of the second order derivatives is used:

$$\frac{\partial^2 N_{ij}}{\partial x^2} = \frac{N^q_{i+1,j} - 2N^q_{i,j} + N^q_{i-1,j}}{\Delta x^2}, \tag{43}$$

$$\frac{\partial^2 N_{ij}}{\partial x \partial y} = \frac{N^q_{i,j} - N^q_{i-1,j} - N^q_{i,j-1} + N^q_{i-1,j-1}}{\Delta x \Delta y}, \quad \text{etc.} \tag{44}$$

This explicit finite differencing is fast (having little impact on computation time) but conditionally stable. Tolman (1995) gives a two-dimensional stability criterion based on Fletcher (1988, Part I, section 7.1.1):

$$Q = \frac{\max(D_{xx}, D_{yy}, D_{xy})\Delta t}{\min(\Delta x, \Delta y)^2} \leq 0.5 \tag{45}$$

Through mathematical analysis (not shown) it can be shown that a likely stability condition for the one-dimensional S&L scheme, with an explicit diffusion term is $\frac{D\Delta t}{\Delta x^2} \leq 0.5$. Thus it is credible that (45) holds true for the two-dimensional S&L scheme, with explicit diffusion. In experiments, we found that for all cases which satisfy the slightly more restrictive $Q \leq 0.48$, no instability was observed. In short, by adding the GSE correction, the unconditionally stable advection equation of SWAN becomes an advection-diffusion equation which is likely conditionally stable. It is readily shown that for typical ocean applications D_{nn} dominates the diffusion Q and can be written as:

$$Q = \bar{C}T/\Delta x \cdot \bar{C}\Delta t/\Delta x \cdot \Delta\theta^2/12. \tag{46}$$

The variable wave age T can be computed during the computations of SWAN (Booij and Holthuijsen, 1987) but it requires the same order of magnitude of computer memory as integrating the action balance equation. Instead a constant wave age $\bar{T}$ can be used as an approximation, so that Eq. (46) becomes

$$Q = \bar{L}/\Delta x \cdot \mu \cdot \Delta\theta^2/12, \tag{47}$$

where the characteristic travel distance of the waves is $\bar{L} = \bar{C}\bar{T}$ (e.g. the dimension of the ocean basin). For oceanic applications the Courant number is at typically $\mu \approx 1/2$ so that $Q \leq 0.25$ for typical values of $\Delta\theta$ and $\bar{L}/\Delta x$ (the number of grid point in one direction of the grid). This implies that the S&L scheme with these GSE-correcting measures is stable for typical ocean cases. For shelf sea (regional) applications the value of $\mu = O(1)$ which is but the garden sprinkler effect tends to be small on these scales and the diffusion can and should be disabled to avoid the stability problem. For small-scale (local) applications typically $\mu = O(10–100)$. But such cases are usually treated as stationary and the SORDUP scheme should be used. An alternative for the GSE-correcting modifications would be to apply a geographic convolution filter on the computational results (a filter that is the equivalent of the diffusion term). This would have the advantage that the nonstationary scheme remains unconditionally stable. (This was not implemented.)

6.4.2. Stationary

GSE corrective measures were not implemented for the SORDUP scheme, as it is unlikely to be a serious problem with stationary simulations (in fact, frequency-related GSE does not occur in stationary simulations).

7. Validation of the improved model

The S&L-based model was validated with a series of tests—described in detail by Rogers et al. (1999)—to confirm that the model performs well under a variety of conditions with and without source terms: idealized simulations, laboratory-scale simulations, and field simulations. The SORDUP model has also been validated (though less extensively than the S&L model).

Stationary computations are generally limited to simulations with smaller domains, since forcing conditions are assumed steady during propagation of wave energy across the domain. For most small scale cases, diffusion will not be a dominant cause of error. For example, in simulations of the DUCK94 experiment (Duck, N.C., Oct 10–22, 1994, with an approximately 2000 km^2 bathymetry grid and uniform wave input; see Rogers et al., 1999), a relatively mild nonuniformity in the wave field is a result of focusing/de-focusing of waves by the bathymetry via refraction. Numerical diffusion tends to smooth such features only slightly. Wave conditions at Duck are typically broad-banded, which tends to mask those numerical errors which do occur. One would expect that the diffusion would have a more pronounced effect on spatial variation of spectral shape than on spatial variation of total energy. Thus, the effect of diffusion for this type of case tends to be subtle and of little interest for many wave model applications.

A small-scale case which is more likely to show greater nonuniformity in an energy field—and thus marked diffusion—is a case of wave blocking by an obstacle such as a breakwater, as shown above. In Section 7.2, we present a small-scale simulation that shares characteristics of the breakwater case: propagation past islands within the Southern California Bight.

Though we do not present the results here, the improved model has been validated in a larger, regional-scale simulation in conjunction with spherical coordinates (N. Booij, personal communication). This was a simulation of nine days during February 1996 in the North Sea (with the computational grid extending from 45°W to 10°E and from 40° to 65° N). Wind forcing and wave buoy data were provided by KNMI (Royal Netherlands Meteorological Office). Time series comparisons at two instrument locations in deep water have the expected trend: results using the S&L scheme show higher peaks and lower troughs, while the results with the first order scheme are noticeably smoothed. The differences are not dramatic (generally less than 5% of the total wave height), because the features being propagated in the wave action field are already relatively smooth and are therefore not greatly diffused by the first order scheme. Judging from comparisons to buoy data, numerical error appears to be small relative to other types, e.g. error associated with forcing and approximations in the model's physics.

7.1. Interaction with source/sink terms and spectral propagation

As has been demonstrated by Tolman (1992), the numerics of geographic propagation can significantly influence the physics of a model. Because source terms and spectral propagation were not included in the mathematical and empirical investigations of the schemes described above, it was necessary to validate the improved model with these components active. Overall, results were quite good, matching results from the original model where appropriate. There was one concern regarding directional spectra output by the model with the S&L scheme: in cases of irregular bathymetry, the directional distributions given by the S&L model tend to be much more irregular than the distributions given by the BSBT model. This is thought to be a result of: 1) interaction between the geographic propagation scheme and the spectral propagation schemes; and, 2) the increased fidelity of the new scheme (which naturally results in larger gradients in the model solution). This increased irregularity does not appear to have a negative impact on the model results in general.

The new schemes appear to work just as well with source terms as they do without. For example, one test combined strong wind input with a "wiggly" S&L scheme solution (intentionally made "wiggly" by using a very large time step size): no unusual behavior was observed. However, it should be mentioned that it is possible—even likely—that numerical analysis performed without regard to source/sink terms will be invalid when these terms are included. Thus it is entirely possible that, strictly speaking, this model remains first order accurate despite implementation of the higher order schemes. This is obviously a concern for a many other types of numerical models. We hope to address the issue in a later study.

7.2. Example field application: Southern California Bight

San Miguel and Santa Rosa Islands are located offshore of Ventura, California, in the Southern California Bight. Fig. 6 shows their location with respect to the coast. The wave climate in the Southern California Bight (stretching from Point

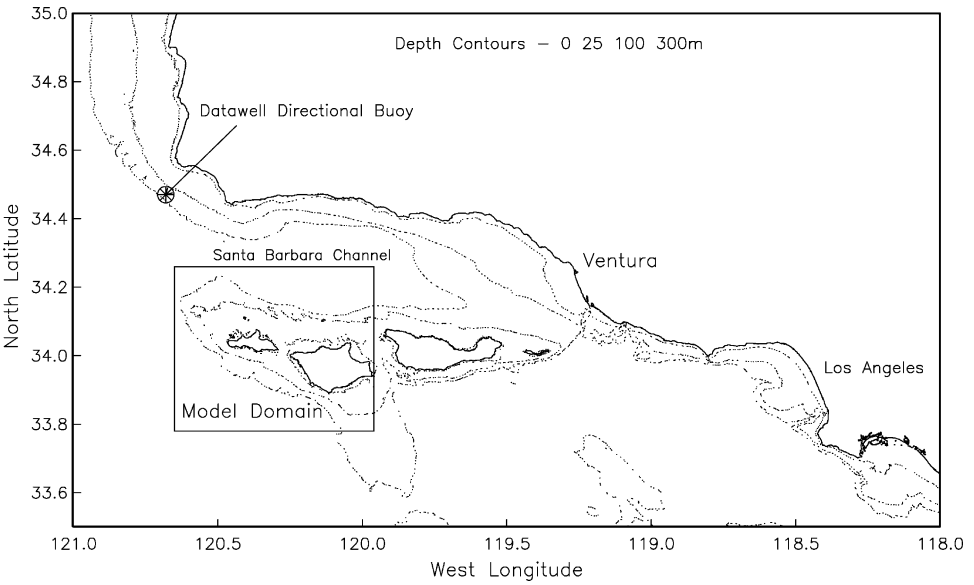

Fig. 6. Map of San Miguel (left) and Santa Rosa (right) Islands and vicinity. The Datawell directional buoy is located at Point Conception. (Figure provided by Dr. W. C. O' Reilly (Scripps)).

Conception south to the Mexican border) has been actively monitored by the Coastal Data Information Program (CDIP), which is based at Scripps Institution of Oceanography in La Jolla. (CDIP is jointly funded by the California Department of Boating and Waterways, and the U.S. Army Corps of Engineers.)

The California shelf is extremely narrow; it is generally no more than 11 km from shoreline to shelf-break. The bathymetry in the Bight is mostly planar, with submarine canyons and other features in some areas. The California coastline south of Point Conception generally faces southwest. The presence of Point Conception shelters much of the Bight from waves coming from the northwest, as occurs often during winter storms. During the summer, the wave climate in the Bight is dominated by swell generated by Southern Hemisphere storms. The islands in the Bight potentially shelter much of the coastline from offshore waves.

In early 1992, pressure gages were installed around the Santa Rosa Island to measure the wave climate in the area. Fig. 7 shows the locations of the gages and the bathymetry around the islands. We will emphasize comparisons of the data with the model at the most sheltered gage, #10. A Datawell buoy located offshore of Point Conception measured waves as they entered the Bight.

7.2.1. Model setup

The computational area for the model is that shown in Fig. 7. The grid extends 66.7 km by 53.4 km, with a resolution of 100 m in both directions. The SWAN model was run on computational grids of four different resolutions: 100, 200, 400, and 800 m. The finest (100 m) resolution allows more direct comparisons to models

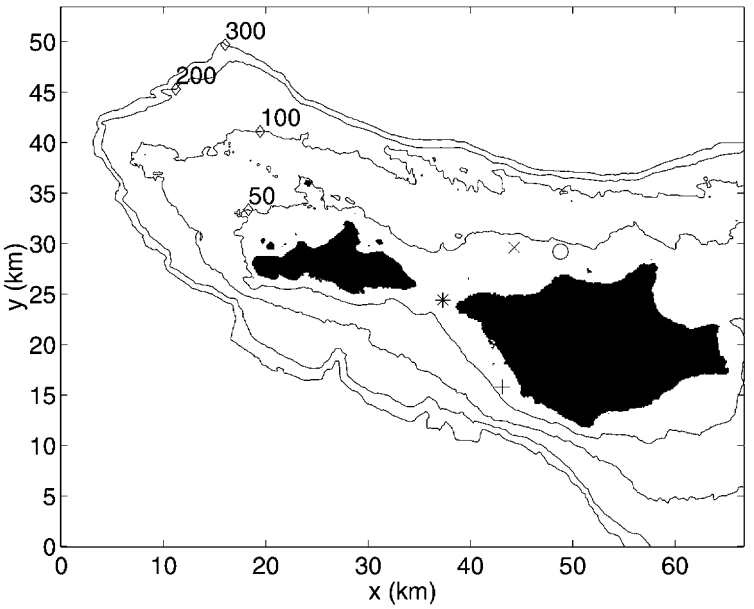

Fig. 7. Bathymetry and gage locations around San Miguel and Santa Rosa Islands. Depths are in meters. Gages shown are: #8 (o), #9 (x), #10 (*), and #11 (+).

run by the Scripps Institution of Oceanography; this resolution also ensures that the bathymetric variations in the vicinity of the islands are well resolved in the model. Directional spectra measured at the Point Conception buoy during January 1992 were used as model input, with data frequencies limited to the swell range (0.05 to 0.09 Hz). The directional range used comprised waves arriving from due north to due south (37 directional bins at 5 degree intervals).

7.2.2. Model results

The SWAN model was run with all January 1992 spectra using the three numerical schemes (pseudo-stationary S&L, stationary BSBT and SORDUP) at the various geographic resolutions. Fig. 8 and Table 1 compare results at identical resolution. Error is calculated using the formula

$$\varepsilon = \left[\frac{\sum_{i=1}^{N} (Z_{pred.} - Z_{meas.})^2}{\sum_{i=1}^{N} Z_{meas.}^2} \right]^{0.5}, \tag{48}$$

where Z is the variable analyzed (in this case, total energy) and N is the number of records in the time series.

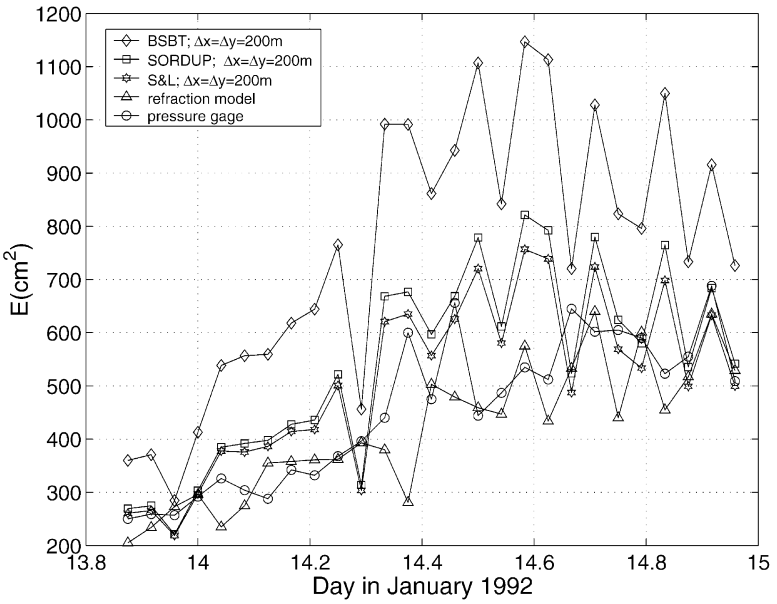

Fig. 8. Time series comparisons of models to data for the Southern California Bight case (total energy is shown). Here, SWAN models of equivalent geographic resolutions are compared at the most sheltered of the pressure gages (#10).

Table 1
Error comparison of models to data for the Southern California Bight case (total energy is shown). SWAN models of equivalent geographic resolutions are compared at gage #10

Model	Geographic resolution (Δx in meters)	Error, ε (of total energy)
Spectral refraction model	100	0.19
SWAN with BSBT scheme	200	0.74
SWAN with SORDUP scheme	200	0.31
SWAN with S&L scheme	200	0.25

Diffusion is manifested as an overprediction of wave energy at this sheltered gage; unsurprisingly, the S&L scheme is most accurate. The SORDUP is nearly as accurate, while the BSBT scheme does poorly. Also shown are results from a ray-based spectral refraction model (LeMehaute and Wang, 1982) run by CDIP (on a 100 m grid), to provide an approximation of what SWAN would produce if no numerical errors were present.

Though Fig. 8 adequately illustrates the relative accuracy of the three schemes, it does not address the issue of efficiency. In fact, though the S&L scheme is more accurate than the stationary schemes for this case, it is more expensive by a factor of 60. This is mostly due to the fact that while the stationary models converges in

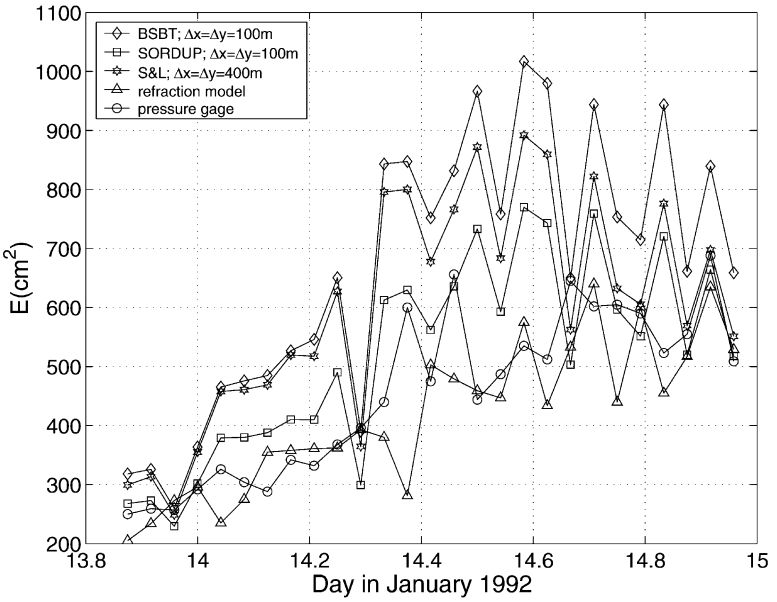

Fig. 9. Time series comparisons of models to data for the Southern California Bight case (total energy is shown). Here SWAN models of approximately equivalent computational requirements are compared at the most sheltered of the pressure gages (#10).

4–5 iterations, the pseudo-stationary model uses 200 time steps to ensure that all spectral components reach steady state. Thus a more fair comparison would be of SWAN models of approximately equal computation time (see Fig. 9 and Table 2). Here, the two stationary models are run on the 100 m grid, while the limit on computation time requires that the S&L model be run on a much coarser grid (400 m). The coarser resolution results in greater diffusion. Thus, in this comparison, the SORDUP scheme is clearly superior. One can expect this to be the case whenever computation time is a concern (i.e. when the number of grid points is not small).

Table 2
Error comparison of models to data for the Southern California Bight case (total energy is shown). SWAN models of approximately equivalent computational requirements are compared at gage #10

Model	Geographic resolution (Δx in meters)	Error, ε (of total energy)
Spectral refraction model	100	0.19
SWAN with BSBT scheme	100	0.55
SWAN with SORDUP scheme	100	0.26
SWAN with S&L scheme	400	0.42

8. Applicability of the implemented schemes

Some general observations can be given regarding the suitability of the three numerical schemes. For oceanic applications, the S&L scheme will almost always be the most effective of the three schemes. At these scales, measures for dealing with the "garden sprinkler effect" are necessary, which unfortunately makes the model conditionally stable like other ocean wave models, e.g. WAM (WAMDI Group, 1988) and WAVEWATCH (Tolman, 1991). Thus higher-order explicit schemes are generally better suited for global-scale wave modeling than the S&L scheme. However, the numerical accuracy of a global wave model with the S&L scheme is much greater than any which uses a first order scheme (implicit or explicit), without a large increase in computational burden (per time step).

For smaller scale, nonstationary models (e.g. regional- and sub-regional- scale modeling), the choice of propagation scheme is somewhat more subjective. At these scales, the GSE correction will typically not be used with the S&L scheme (for example, no GSE was noticed the simulation of the North Atlantic discussed earlier), so there is no "hard" stability criterion for the scheme. However, there is a soft CFL criterion, typically in the range of 2–10, necessary to prevent non-physical oscillations ("wiggles"). The limiting number used is dependent on the tolerance of the user and the resolution of spatial gradients by the computational grid. For finely resolved grids, this limits the size of the time step that can be safely used with the S&L scheme. This is in contrast to the BSBT scheme, for which a large time step can be used without an obvious penalty. Thus, scheme choice depends on the "natural" time step size of the simulation, determined by factors such as the time increment of forcing data, the step size required for proper behavior of source/sink terms, etc. In cases where the S&L scheme dictates a smaller time step size, this cost must be weighed against likely benefit. The benefit of a higher order scheme is obviously greater for cases that are prone to diffusion. What constitutes "diffusion-prone" is not obvious. The degree of nonuniformity (or, more specifically, the leading even-ordered terms in a scheme's truncation error) provides a general sense of whether a particular model application is prone to diffusion. A more definitive measure of diffusion-proneness is unfortunately impractical.

A significant advantage of a soft CFL criterion, as compared to the hard stability criterion of a conditionally stable model, is that the modeler has the freedom to choose the time step according to the peak frequency component rather than according to the lowest frequency component. Similarly, in the case of curvilinear grid applications, the smallest geographic resolution in the grid does not dictate the time step used for the entire simulation. Thus, the S&L is better suited for many regional scale applications than would be a conditionally stable, high-order, explicit scheme.

For stationary cases, any of the three schemes (S&L, SORDUP, BSBT) can be used. However, the SORDUP scheme will almost always be the best choice in terms of efficiency, for reasons discussed previously:

1. the SORDUP scheme is more accurate (less diffusive) than the BSBT scheme,

only slightly more expensive, and non-physical oscillations are generally mild and avoidable.
2. the SORDUP scheme is almost as accurate at the S&L scheme, and is typically much less expensive for moderate to large grids (10000 or more grid points) than the S&L scheme.

9. Summary

In order to reduce numerical diffusion in the third generation wave model SWAN, two second order finite differencing schemes, denoted as "S&L" (from Stelling and Leendertse, 1992) and "SORDUP" (Second ORDer, UPwind), have been implemented in the geographic propagation routine of the model and will be available as options in a future public release of the code. These two schemes were chosen after extensive mathematical analysis and numerical experimentation with a number of schemes. In this paper, we present notable aspects of these investigations, including that of the pre-existing, first order "BSBT" (Backward Space, Backward Time) scheme, and three schemes which were not implemented in the full version of the code, but are noteworthy enough to be included in the discussion: "NISL" (Non-Interpolating, Semi-Lagrangian, Olim 1994), "BCML (n=3)" (Backward Characteristic Method, Lagrangian interpolation), and the "Box" scheme. The improved model has been validated. It demontrates greatly reduced diffusion in cases where diffusion presents problems with the original model. One validation exercise was described herein: a simulation of swell propagation past islands in the Southern California Bight. Results (at a location in the grid that is conducive to diffusion) are dramatically improved with the higher order schemes.

To further accommodate application at larger scales, for which the curvature of the earth is of significance, the model has been reformulated in spherical coordinates. This has been demonstrated, alongside the two implemented higher order schemes, in Holthuijsen and Booij (2000).

All three schemes appear to be unconditionally stable and action-conserving in the general case of nonuniform Courant number. In the context of a wave action model, this suggests than they can be safely applied in the presence of nonuniform bathymetry and current field. None of the schemes are superior to the others in all modeling situations; we have discussed the applicability and efficiency of each scheme. By carefully choosing the scheme appropriate for a given situation, the SWAN model can be used to model wind waves at any scale with relatively minimal numerical error.

Acknowledgements

Dr. W.C. O'Reilly (Scripps Institute of Oceanography) provided the Southern California Bight test case (including bathymetry, buoy and pressure gage data, and SIO model results) and acted as lead Principal Investigator of this project. Thanks to

Larry Hsu of the U.S. Naval Research Laboratory for his participation. The authors would also like to thank Guus Stelling (Technical University of Delft) and Moshe Olim (FSI International) for taking time to discuss their numerical schemes. We would also like to acknowledge the contribution of many unpublished (and mostly anonymous) sources from which the third author (H.P.) obtained his collection of numerical schemes that formed the base of this study. Wind and wave data used in the North Atlantic application were used with permission from KNMI (Royal Netherlands Meteorological Office). The ONR Advanced Wave Prediction Program has funded this work (ONR Grant N00014-98-1-0010, NRL Contribution JA/7320—01-0002).

References

Bender, L.C., 1996. Modification of the physics and numerics in a third-generation ocean wave model. J. Atm. and Oceanic Tech. 13, 726–750.

Booij, N., Holthuijsen, L.H., 1987. Propagation of ocean waves in discrete spectral wave models. J. of Comput. Physics 68, 307–326.

Booij, N., Ris, R.C., Holthuijsen, L.H., 1999. A third generation wave model for coastal regions; Part I: model description and validation. J. of Geophysical Res. 104, 7649–7666.

Davis, R.W., Moore, E.F., 1982. A numerical study of vortex shedding from rectangles. J. Fluid Mech. 116, 475–506.

Fletcher, C.A.J., 1988. Computational Techniques for Fluid Dynamics, Parts I and II. Springer,

Hasselmann, K., Barnett, T.P., Bouws, E., Carlson, H., Cartwright, D.E., Enke, K., Ewing, J.A., Gienapp, H., Hasselman, D.E., Kruseman, P., Meerburg, A., Muller, P., Olbers, D.J., Richter, K., Sell, W., Walden, H., 1973. Measurements of wind-wave growth and swell decay during the Joint North Sea Wave Project (JONSWAP). Dtsch. Hydrogr. Z. Suppl. 12, 1–95.

Hardy, T.A., Mason, L.B., McConochie, J.D., 2000. A wave model for the Great Barrier Reef. Ocean Eng. 28, 45–70.

Holthuijsen. L.H., Booij, N., 2000. Oceanic and near-shore whitecapping effects in SWAN, in Proc. 6th Intern. Workshop on Wave Hindcasting and Forecasting, Monterey, CA, USA, Nov 2000. (Meteorological Service of Canada, Downsview, Canada), pp. 362–368.

Le Mehaute, B., Wang, J.D., 1982. Wave spectrum changes on sloped beach. ASCE J. Waterways Port Coast and Ocean Engineering 108, 33–47.

Leonard, B.P., 1979. A stable and accurate convective modeling procedure based on quadratic upstream interpolation. Computer Methods in Applied Mechanics and Engineering 19, 59–98.

Leonard, B.P., 1991. The ULTIMATE conservative difference scheme applied to unsteady one-dimensional advection. Comput. Methods Appl. Mech. Eng. 88, 17–74.

Lin, R.Q., Huang, N.E., 1996. The Goddard Coastal Wave Model Part I: numerical method. J. of Phys. Oceanog. 26, 833–847.

Mei, C.C., 1983. The Applied Dynamics of Ocean Surface Waves. Wiley, New York.

Neu, W.L., Won, Y.S., 1990. Propagation schemes for wind wave models with finite depth and current. In: Rahman, M. (Ed.), Ocean Wave Mechanics, Computational Fluid Dynamics and Mathematical Modeling, pp. 947–954.

Olim, M., 1994. A Truly Noninterpolating Semi-Lagrangian Lax–Wendroff Method. J. of Comp. Phys. 112, 253.

Petit, H., 1997. Dissipation and Dispersion of Numerical Schemes for Hyperbolic Problems. Delft Hydraulics,

Philips, O.M., 1977. The Dynamics of the Upper Ocean. Cambridge University Press,

Preissman, A., 1961. Propagation of translatory waves in channels and rivers; (in French), Proc., First Congress of French Association for Compuation (AFCAL), Grenoble, France, 433–442.

Ris, R.C., 1997. Spectral Modeling of Wind Waves in Coastal Areas. Report no. 97-4, Department of Civil Engineering, Delft University of Technology.

Rogers, W.E., Kaihatu, J.M., Booij, N., Holthuijsen, N., 1999. Improving the Numerics of a Third-Generation Wave Action Model. NRL Formal Report 7320-99-9695, 79 pp.

Stelling, G.S., Leendertse, J.J., 1992. Approximation of convective processes by cyclic AOI methods. Proceedings, 2nd International Conference on Estuarine and Coastal Modeling, Tampa, Florida, ASCE, 771–782.

SWAMP Group 1985. Ocean Wave Modeling. Plenum, New York.

Tolman, H.L., 1991. A third generation model for wind waves on slowly varying unsteady and inhomogeneous depths and currents. J. Phys. Oceanogr. 21, 782–797.

Tolman, H.L., 1992. Effects of numerics on the physics in a third-generation wind-wave model. J. Phys. Oceanogr. 22, 1095–1111.

Tolman, H.L., 1995. On the selection of propagation schemes for a spectral wind-wave model. NWS/NCEP Office Note 411, 30 pp. + figures.

WAMDI Group, 1988 1988. WAM model A third generation wave prediction model. J. Phys. Oceanography 18, 1775–1810.

Whitham, G.B., 1974. Linear and Nonlinear Waves. Wiley, New York.